Neuron
Article

Endocannabinoids Mediate Neuron-Astrocyte Communication

Marta Navarrete[1] and Alfonso Araque[1,*]
[1]Instituto Cajal, Consejo Superior de Investigaciones Científicas, Madrid 28002, Spain
*Correspondence: araque@cajal.csic.es
DOI 10.1016/j.neuron.2008.01.029

SUMMARY

Cannabinoid receptors play key roles in brain function, and cannabinoid effects in brain physiology and drug-related behavior are thought to be mediated by receptors present in neurons. Neuron-astrocyte communication relies on the expression by astrocytes of neurotransmitter receptors. Yet, the expression of cannabinoid receptors by astrocytes in situ and their involvement in the neuron-astrocyte communication remain largely unknown. We show that hippocampal astrocytes express CB1 receptors that upon activation lead to phospholipase C-dependent Ca^{2+} mobilization from internal stores. These receptors are activated by endocannabinoids released by neurons, increasing astrocyte Ca^{2+} levels, which stimulate glutamate release that activates NMDA receptors in pyramidal neurons. These results demonstrate the existence of endocannabinoid-mediated neuron-astrocyte communication, revealing that astrocytes are targets of cannabinoids and might therefore participate in the physiology of cannabinoid-related addiction. They also reveal the existence of an endocannabinoid-glutamate signaling pathway where astrocytes serve as a bridge for nonsynaptic interneuronal communication.

INTRODUCTION

Recent evidence has demonstrated the existence of bidirectional communication between astrocytes and neurons (Araque et al., 2001; Haydon and Carmignoto, 2006; Nedergaard et al., 2003; Volterra and Bezzi, 2002). Astrocytes respond with intracellular Ca^{2+} elevations to neurotransmitters released by synaptic terminals (Perea and Araque, 2005; Porter and McCarthy, 1996) and, in turn, modulate neuronal excitability and synaptic transmission by releasing neuroactive substances called gliotransmitters (Araque et al., 1999; Beattie et al., 2002; Perea and Araque, 2007; Volterra and Bezzi, 2002). Neuron-to-astrocyte communication is based on the expression by astrocytes of different neurotransmitter receptors that, in many cases, are coupled to second messenger pathways that upon activation lead to mobilization of Ca^{2+} from the intracellular stores. The presence of cannabinoid receptors in astrocytes is controversial (for a review see Stella, 2004). While some studies did not detect cannabinoid effects on astrocytes, cannabinoid receptors have been ultrastructurally localized in astrocytes of the caudate putamen nucleus (Rodriguez et al., 2001) and the dorsal horn of the spinal cord (Salio et al., 2002), and several studies have shown their presence in cultured glial cells (Molina-Holgado et al., 2003; Stella, 2004; Walter and Stella, 2003). Consequently, the expression of functional cannabinoid receptors by astrocytes in situ remains poorly defined, and their involvement in the neuron-astrocyte communication is unknown.

The endocannabinoid system is an important intercellular signaling system involved in a wide variety of physiological processes. It consists of cannabinoid receptors, endogenous transmitters (called endocannabinoids), and the enzymatic machinery for their synthesis, release, and degradation. Two types of cannabinoid receptors, termed CB1Rs and CB2Rs, have been characterized, and the existence of additional receptors has been suggested (Matsuda et al., 1990; Munro et al., 1993). While CB2Rs are mainly expressed by cells of the immune system, CB1Rs are highly expressed in many brain regions, where they play relevant neuromodulatory roles in brain physiology (Chevaleyre et al., 2006; Freund et al., 2003; Rodriguez et al., 2001). CB1Rs mediate retrograde inhibition of transmitter release, control neuronal excitability, and regulate short- and long-term synaptic plasticity (Alger, 2002; Chevaleyre et al., 2006; Freund et al., 2003; Kreitzer and Regehr, 2002; Wilson and Nicoll, 2002). Furthermore, these receptors are responsible for most of the psychotropic and behavioral effects of cannabinoids (Maldonado et al., 2006; Di Marzo et al., 2004). Cannabinoid effects in brain physiology are thought to be mediated by CB1Rs exclusively present in neurons. Indeed, numerous studies have focused on the CB1 expression by different subpopulations of neurons in different brain areas, but the possible functional expression of cannabinoid receptors by astrocytes in situ has been largely disregarded.

The identification of all of the cellular mechanisms involved in cannabinoid signaling is essential for a full understanding of its cellular bases and physiological consequences. Therefore, we used electrophysiological and Ca^{2+} imaging techniques in mice brain slices to investigate the functional expression of cannabinoid receptors by hippocampal astrocytes and their participation in the neuron-astrocyte communication. We found that hippocampal astrocytes express functional CB1Rs, which upon activation lead to phospholipase C-dependent Ca^{2+} mobilization from internal stores. These receptors can be activated by endocannabinoids released from pyramidal neurons, increasing the astrocyte Ca^{2+} levels and stimulating the release of glutamate,

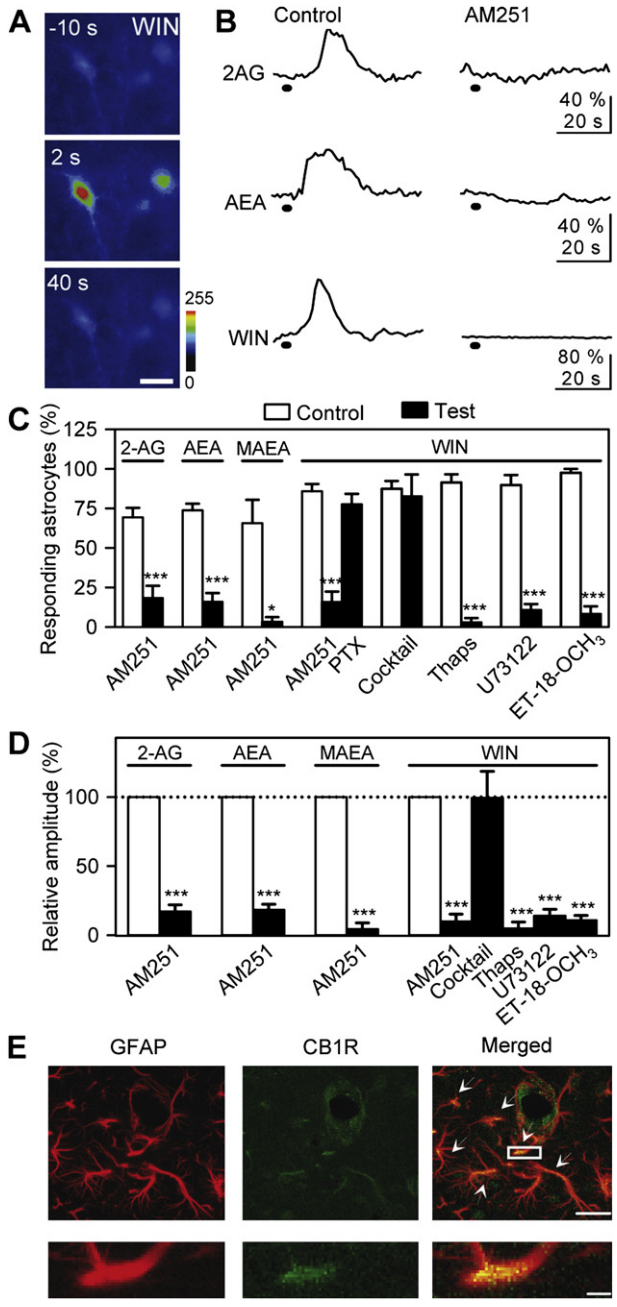

Figure 1. Cannabinoid Receptor Activation Increases Ca^{2+} Levels in Astrocytes

(A) Pseudocolor images representing fluorescence intensities of a fluo-4-filled hippocampal astrocyte of CA1 stratum radiatum 10 s before and 2 and 40 s after local application of WIN delivered by pressure pulse from a micropipette. Scale bar, 15 μm.

(B) Astrocytic Ca^{2+} levels evoked by local application (horizontal bars) of 2AG, AEA, and WIN in control and 2 μM AM251.

(C and D) Proportion of responding astrocytes and relative fluorescence changes induced by CB1R agonists in control (white bars) and test conditions (black bars). The cocktail contained TTX and glutamatergic, GABAergic, cholinergic, and purinergic receptor antagonists (see Results). Each bar, ≥30 astrocytes from n ≥ 4 slices. Error bars indicate SEM. Significant differences were established at *$p < 0.05$ and ***$p < 0.001$.

(E) Immunocytochemical localization of GFAP and CB1R in stratum radiatum hippocampal astrocytes. Top images show staining for GFAP and CB1R and their colocalization (left to right). The astrocytic process marked with a box in the merged image was magnified (bottom images). Images were obtained by laser-scanning confocal microscopy constructed from a stack of four successive images (1 μm deep). Scale bars, 20 and 3 μm (top and bottom, respectively).

which signals back to neurons activating NMDARs, evoking slow inward current in pyramidal neurons.

RESULTS

Hippocampal Astrocytes Express Functional Endocannabinoid Receptors that Mediate Intracellular Calcium Elevations

To investigate whether hippocampal astrocytes express functional endocannabinoid receptors, we recorded the intracellular Ca^{2+} levels of astrocytes located in the stratum radiatum of the CA1 region and analyzed the responses to local application of endogenous as well as synthetic agonists of these receptors. Local application of 2-arachidonylglycerol (2AG), arachidonylethanolamide (AEA), (R)-(+)-methanandamide (MAEA), or (*R*)-(+)-WIN 55,212-2 (WIN) by pressure pulses through a micropipette increased the intracellular Ca^{2+} levels in 125 out of 169 astrocytes (from a representative sample of n = 21 slices; Figures 1A–1C). The number of responding astrocytes and the relative fluorescence change evoked by the agonists were inhibited by the selective antagonist of CB1Rs, AM251 (2 μM; Figures 1B–1D and Figure S1A available online), indicating that the observed Ca^{2+} elevations were mediated by CB1R activation.

Astrocytic responses could be indirectly evoked by CB1R agonists because CB1Rs are largely present in glutamatergic and GABAergic synaptic terminals where they can inhibit synaptic transmitter release (Alger, 2002; Chevaleyre et al., 2006; Freund et al., 2003; Llano et al., 1991; Rodriguez et al., 2001). Therefore, we analyzed the astrocytic responses to the local application of the CB1R agonist WIN before and after blocking glutamatergic, GABAergic, cholinergic, and purinergic receptors with a cocktail containing CNQX (20 μM; for AMPA and kainate glutamate receptors), AP5 (50 μM; for NMDA glutamate receptors), MPEP (50 μM; for metabotropic glutamate receptors mGluR5), LY367385 (100 μM; for metabotropic glutamate receptors mGluR1), picrotoxin (50 μM; for $GABA_A$ receptors), saclofen (100 μM; for $GABA_B$ receptors), atropine (50 μM; for muscarinic cholinergic receptors), CPT (10 μM; for A1 adenosine receptors), and suramin (100 μM; for P2 purinergic receptors). The cocktail also contained TTX (1 μM) to prevent action potential-mediated neurotransmitter release. The proportion of responding astrocytes and the amplitude of the WIN-evoked Ca^{2+} elevations were not significantly affected by the cocktail of receptor antagonists, suggesting that the observed responses were directly mediated by CB1R activation in astrocytes. Furthermore, Ca^{2+} elevations in response to WIN were absent in 27 out of 30 astrocytes tested in five hippocampal slices from transgenic mice lacking CB1R expression (Zimmer et al., 1999) (Figure 2). These astrocytes were able to respond with Ca^{2+} elevations to ATP application, indicating that transmitter receptor-mediated Ca^{2+}

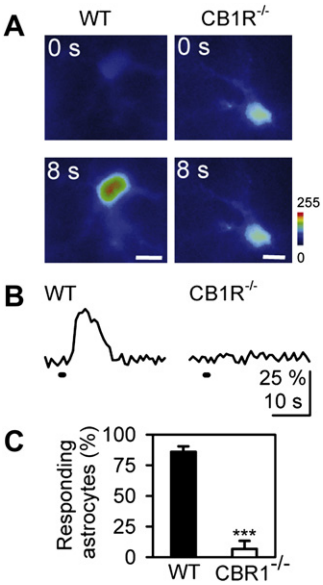

Figure 2. Astrocyte Ca^{2+} Levels Are Unaffected by Cannabinoids in *CB1R*$^{-/-}$ Mice

(A) Pseudocolor images representing fluorescence intensities of fluo-4-filled astrocytes in hippocampal slices from wild-type and *CB1R*$^{-/-}$ mice before and 8 s after local application of WIN. Scale bars, 7 μm.

(B) Astrocyte Ca^{2+} levels evoked by local application of WIN (horizontal bars), in wild-type and *CB1R*$^{-/-}$ mice.

(C) Proportion of responding astrocytes to WIN application in wild-type and *CB1R*$^{-/-}$ mice. Each bar, ≥30 astrocytes from n ≥ 8 slices. Error bars indicate SEM. Significant differences were established at ***$p < 0.001$.

mobilization was not impaired in astrocytes from *CB1*$^{-/-}$ mutant mice (22 out of 23 astrocytes; data not shown). This result confirms that CB1Rs were responsible for the observed astrocytic Ca^{2+} elevations.

Astrocytes express a wide variety of receptors for many neurotransmitters, and some of them are coupled to different G proteins (Porter and McCarthy, 1997). CB1Rs are mainly coupled to pertussis toxin (PTX)-sensitive $G_{i/o}$ proteins that regulate cAMP levels. In addition, a recent report indicates that these receptors can also be coupled to $G_{q/11}$ proteins that activate PLC (Lauckner et al., 2005). We used pharmacological tools to investigate the intracellular signaling pathway involved in the CB1R-mediated astrocytic responses. First, we investigated the nature of the G protein involved by incubating the slices with 7.5 μg/ml PTX for 4–8 hr and analyzing the astrocyte Ca^{2+} signal. To asses the effectiveness of PTX treatment, we first applied GABA, which evokes Ca^{2+} elevations mediated by $GABA_B$ receptors (Kang et al., 1998; Serrano et al., 2006), which are known to be coupled to $G_{i/o}$ proteins (Catsicas and Mobbs, 2001). GABA-evoked Ca^{2+} elevations regularly observed in control slices (21 out of 38 astrocytes from seven slices) were absent in 24 out of 29 astrocytes from four slices pretreated with PTX (data not shown). In contrast, in those PTX-treated slices, the proportion of astrocytes that responded with Ca^{2+} elevations to local application of WIN was similar to control slices (Figure 1C), indicating that CB1R-induced astrocyte Ca^{2+} signal was not mediated by PTX-sensitive G proteins.

Next, we analyzed the participation of the intracellular Ca^{2+} stores by perfusing the slices with thapsigargin, which depletes them by inhibiting the Ca^{2+} ATPase (Araque et al., 1998). After control recordings, the slices were perfused with 1 μM thapsigargin for 30–45 min. The WIN-evoked astrocytic Ca^{2+} elevations were diminished by thapsigargin (Figure 1C), indicating that they require the presence of intact intracellular Ca^{2+} stores. The PLC antagonists U73122 (4 μM) and ET-18-OCH3 (15 μM) also decreased the WIN-evoked Ca^{2+} elevations (Figure 1D), indicating that Ca^{2+} elevations evoked by cannabinoids in astrocytes are mediated by CB1Rs that activate PLC, probably through a $G_{q/11}$ protein, and mobilize Ca^{2+} from internal stores.

Besides the functional expression of CB1Rs in astrocytes, to obtain morphological evidence of CB1R presence in astrocytes, we performed immunocytochemical analysis using antibodies against CB1Rs and GFAP (a specific marker of astrocytes). CB1R signal could be observed in astrocytic processes identified by their GFAP staining in stratum radiatum hippocampal astrocytes (Figure 1E).

Astrocytes Respond with Intracellular Calcium Elevations to Neuronal Depolarization

Hippocampal pyramidal neurons are known to be a source of endocannabinoids that can be released under different experimental conditions, such as neuronal depolarization or postsynaptic metabotropic glutamate receptor activation (Alger, 2002; Chevaleyre et al., 2006; Kreitzer and Regehr, 2002). We therefore investigated whether the CB1R-mediated intracellular Ca^{2+} signal in astrocytes can be endogenously evoked by endocannabinoids released from CA1 pyramidal neurons. We electrophysiologically recorded CA1 pyramidal neurons, monitored Ca^{2+} levels in adjacent astrocytes (within a 150 μm wide region perpendicular to the stratum pyramidale), and depolarized the neuron to 0 mV to stimulate endocannabinoid release (Chevaleyre and Castillo, 2003; Kreitzer and Regehr, 2001; Ohno-Shosaku et al., 2001; Wilson and Nicoll, 2001).

In relatively quiescent astrocytes, neuronal depolarization (ND) evoked a slow, transient Ca^{2+} elevation in adjacent astrocytes (17 out of 31 astrocytes from four slices; see Movie S1). These astrocytic responses could be reliably evoked by successive neuronal stimuli and were reversibly abolished by 2 μM AM251 (n = 13; Figure 3B). Most hippocampal astrocytes display spontaneous Ca^{2+} oscillations that can be modulated by different neurotransmitters (Nett et al., 2002; Perea and Araque, 2005). We therefore analyzed the effects of neuronal depolarization (ND) on the Ca^{2+} signal of several astrocytes in the field of view (from 8 to 14 astrocytes), quantifying two parameters, i.e., the probability of occurrence of a Ca^{2+} elevation (Ca^{2+} spike) and the mean frequency oscillation 50 s before (basal) and after the onset of the ND (Figures 3C–3G). In 11 hippocampal slices, 49% ± 4% of the astrocytes increased their Ca^{2+} oscillation frequency after neuronal depolarization (Figures 3F and 3G), while the relative mean amplitudes of the Ca^{2+} elevations were unchanged (mean amplitude of the Ca^{2+} signal during ND was 86.1% ± 13.1% relative to corresponding basal amplitudes). Furthermore, the Ca^{2+} spike probability was transiently increased by ND (n = 7; Figure 3E). These effects could be consistently evoked by successive neuronal stimuli (Figure 4A) and depended on the

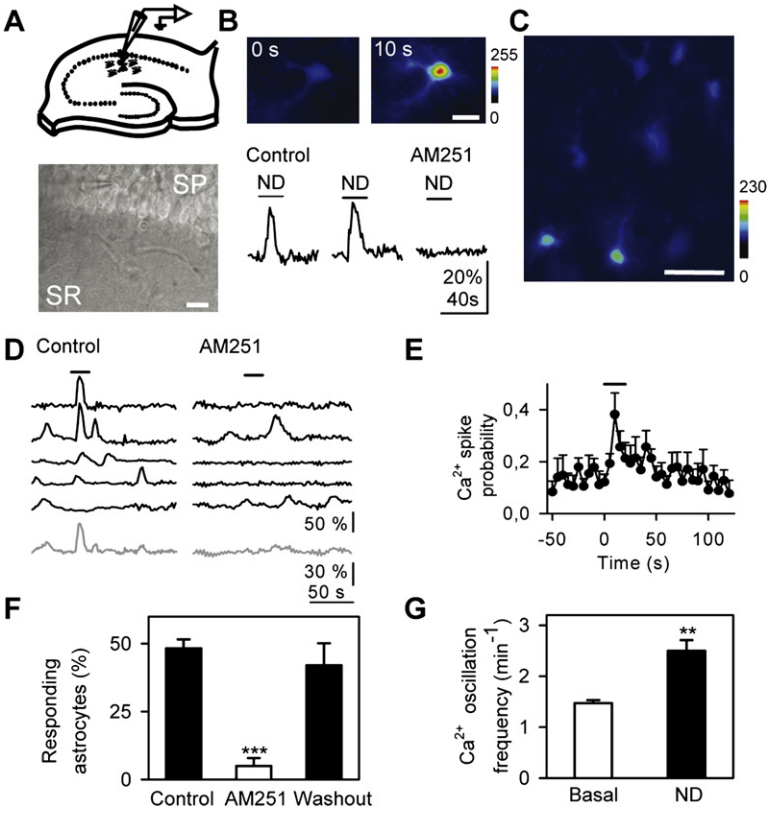

Figure 3. Neuronal Depolarization Increases Ca^{2+} Signal in Hippocampal Astrocytes

(A) Schematic drawing and infrared differential interference contrast image showing the stratum radiatum (SR) and the recorded neuron in the stratum pyramidale (SP). Scale bar, 20 μm.

(B) (Top) Pseudocolor images representing astrocyte fluorescence intensities before and after neuronal depolarization (ND); (bottom) astrocyte Ca^{2+} levels evoked by ND (horizontal bars) in control and AM251. Scale bar, 15 μm.

(C) Pseudocolor image of a representative field of view showing eight hippocampal astrocytes in the stratum radiatum. Scale bar, 40 μm.

(D) Ca^{2+} levels from five astrocytes in a field of view and corresponding average traces (gray) in control and AM251. Horizontal bars indicate ND.

(E) Astrocyte Ca^{2+} spike probability versus time (n = 7 slices). Time 0 corresponds to the beginning of the ND.

(F) Relative number of astrocytes that increased their Ca^{2+} oscillation by ND in control, AM251, and after washout (n = 37 astrocytes from four slices).

(G) Mean Ca^{2+} oscillation frequency before (basal) and after ND. Error bars indicate SEM. Significant differences were established at $^{**}p < 0.01$ and $^{***}p < 0.001$.

depolarizing pulse duration (Figures S1B and S1C). Taken together, these results indicate that neuronal depolarization modulates the Ca^{2+} signal of adjacent astrocytes, evoking intracellular Ca^{2+} elevations in relatively silent astrocytes, increasing the oscillation frequency of oscillating astrocytes, and increasing the probability of occurrence of Ca^{2+} elevations.

Interestingly, while most astrocytes showed Ca^{2+} elevations upon exogenous local stimulation with cannabinoids (85.8% ± 4.5% of 42 astrocytes from six slices, see Figure 1), astrocytic Ca^{2+} signal modulation by ND was observed in a subset of astrocytes (49.2% ± 4.0% of 105 astrocytes from 11 slices). However, astrocytes consistently responded or not to the successive stimulation of a given neuron, i.e., astrocytes responding to the first ND also responded to the second ND, while nonresponding astrocytes to the first stimulus did not respond to the second ND either (Figure 4B). Furthermore, nonresponding astrocytes to ND were able to respond with Ca^{2+} elevations upon exogenous stimulation with WIN (16 out of 18 astrocytes from four slices; data not shown). These results indicate that astrocytic responses did not result from a wide spillover of endocannabinoids and suggest the existence of intercellular signaling endocannabinoid pathways between neurons and astrocytes.

Because endocannabinoid signaling might be affected by temperature (Kreitzer et al., 2002), we investigated whether astrocytic responses to endocannabinoids were also present at more physiological temperature (34°C). The increase of the Ca^{2+} spike probability and the Ca^{2+} oscillation frequency evoked by ND, as well as the proportion of responding astrocytes (55% ± 3% at 24°C and 57% ± 6% at 34°C), were not significantly different at 24°C and 34°C (n = 48 astrocytes from six slices) (Figure 4C), indicating that endocannabinoid-mediated neuron-astrocyte signaling occurs under physiological conditions.

Endocannabinoids Released by Pyramidal Neurons Evoke Astrocyte Calcium Elevations

To investigate the cellular mechanisms involved in the ND-evoked astrocytic Ca^{2+} elevation, we compared the astrocyte Ca^{2+} signal parameters (i.e., Ca^{2+} oscillation frequency and probability of Ca^{2+} elevation) before and after different pharmacological treatments (Figures 4D and 4E). The ND-evoked increase of the astrocyte Ca^{2+} signal was not prevented in the presence of TTX or after dialyzing the stimulating neuron with QX-314, which intracellularly blocks voltage-gated Na^+ currents, suggesting that the observed effects of ND were not due to action potential-mediated neural network activation. Consistent with results obtained by local application of CB1R agonists, ND-evoked increases in both Ca^{2+} oscillation frequency and Ca^{2+} elevation probability were unaffected in the presence of the cocktail of neurotransmitter receptor antagonists, but they were abolished by the CB1R antagonist AM251 (2 μM). In agreement with these results, modulation of the astrocyte Ca^{2+} signal by ND was not observed in slices from *CB1R*$^{-/-}$ transgenic mice (n = 34 astrocytes from five slices; Figures 4D and 4E), indicating that the increase of the astrocyte Ca^{2+} oscillations evoked by ND was selectively mediated by CB1R activation.

To investigate the intracellular signaling pathway involved, we incubated the slices with 7.5 μg/ml PTX. After assessing the effectiveness of PTX treatment by confirming the absence of astrocyte

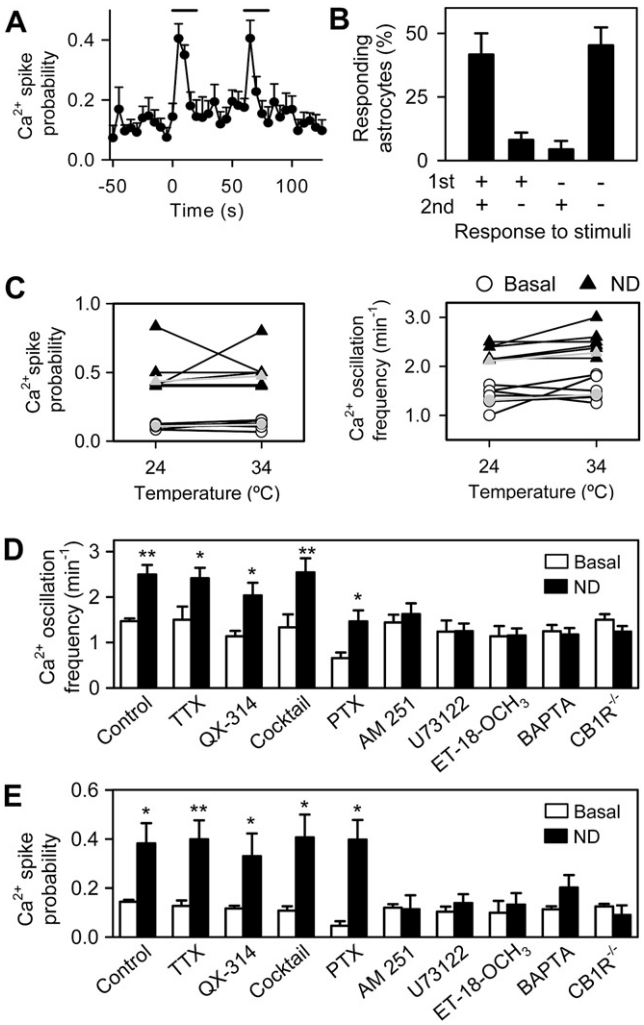

Figure 4. Astrocytic Ca^{2+} Elevations Evoked by Neuronal Depolarization Are Mediated by CB1R Activation

(A) Astrocyte Ca^{2+} spike probability evoked by successive ND (horizontal bars) (n = 37 astrocytes from four slices).

(B) Proportion of astrocytes that responded to two successive ND. Note that almost all of the astrocytes either responded (+) or not (–) to the first and second stimuli (n = 123 astrocytes from ten slices).

(C) Astrocyte Ca^{2+} spike probability and Ca^{2+} oscillation frequency before (basal; open symbols) and after neuronal depolarization (ND; filled symbols) at 24°C and 34°C (48 astrocytes from six slices). Gray symbols indicate mean values.

(D and E) Astrocyte Ca^{2+} oscillation frequency and Ca^{2+} spike probability, respectively, before (basal; white bars) and after neuronal depolarization (ND; black bars) in control and test conditions ($n \geq 5$ slices for each bar). Error bars indicate SEM. Significant differences were established at $^{*}p < 0.05$, $^{**}p < 0.01$.

Ca^{2+} elevations in response to ionophoretical application of GABA (31 out of 36 astrocytes from five slices did not respond to GABA; data not shown), we tested the effects of ND on the astrocyte Ca^{2+} oscillations. Although a slight reduction of the basal oscillation frequency was observed in PTX-treated slices (probably due to the deleterious effects of PTX on cellular viability), both the Ca^{2+} oscillation frequency and the Ca^{2+} spike probability were significantly increased after neuronal depolarization (Figures 4D and 4E). In contrast, the PLC antagonists U73122 (4 μM) and ET-18-OCH3 (15 μM) abolished the astrocytic response to ND. Taken together, these results indicate that the intracellular Ca^{2+} elevations evoked in astrocytes by ND are mediated by CB1R activation that stimulates PLC.

We then investigated whether the ND-induced increase of the astrocyte Ca^{2+} signal was mediated by endocannabinoids released from pyramidal neurons. Neuronal depolarization stimulates the release of endocannabinoids, which transiently reduces inhibitory transmitter release by activation of presynaptic CB1Rs, a process known as depolarization-induced suppression of inhibition (DSI) (for review see Alger 2002; Freund et al., 2003; Chevaleyre et al., 2006). Using DSI as bioassay for endocannabinoid release, we compared the effects of ND on the DSI in neurons and the Ca^{2+} spike probability in astrocytes by simultaneously recording inhibitory postsynaptic currents (IPSCs) from pyramidal neurons and astrocyte Ca^{2+} levels (Figures 5A and 5B). Increasing the duration of the ND induced a gradual increase of both the proportion of DSI and the astrocyte Ca^{2+} spike probability (Figures 5C and 5D). Both parameters showed a high degree of correlation ($r^2 = 0.83$). These results suggest that astrocyte Ca^{2+} signal results from endocannabinoids released from pyramidal neurons and indicate that endocannabinoids are similarly effective in inducing neuronal and astrocytic effects.

Because endocannabinoid release by neuronal depolarization requires the increase of neuronal intracellular Ca^{2+} (Chevaleyre and Castillo, 2003; Kreitzer and Regehr, 2001; Ohno-Shosaku et al., 2001; Wilson and Nicoll, 2001), to further test the idea that astrocyte Ca^{2+} elevations were induced by endocannabinoids released by neurons, we selectively manipulated the intracellular Ca^{2+} levels in the pyramidal neuron. First, we performed paired whole-cell recordings from two adjacent pyramidal neurons (Figures 6A and 6B). One recording pipette included the Ca^{2+} chelator BAPTA (20 mM) to prevent Ca^{2+} rises in one pyramidal neuron, while the other neuron, filled with standard intracellular solution, was used as a control. While depolarization of the control neuron increased both the Ca^{2+} spike probability and the Ca^{2+} oscillation frequency in astrocytes, depolarization of the BAPTA-filled neuron did not affect the astrocyte Ca^{2+} signal (Figure 6B). Second, in another set of experiments, the recorded neuron was loaded through the recording pipette with the Ca^{2+}-cage NP-EGTA to selectively increase its Ca^{2+} levels after UV-flash photolysis stimulation. These experiments were performed in the presence of TTX to prevent action potential-evoked neurotransmitter release. UV-flash stimulation elevated neuronal Ca^{2+} and increased the astrocyte Ca^{2+} spike probability (Figures 6C–6F). In the absence of NP-EGTA-loaded neurons, UV-flashes did not modify astrocyte Ca^{2+} levels (Figure 6F), indicating that the effects were not due to direct photostimulation of astrocytes.

Taken together, these results indicate that Ca^{2+} elevations in pyramidal neurons are necessary and sufficient to induce Ca^{2+} elevations in astrocytes and further support the idea that the CB1R-mediated astrocyte Ca^{2+} responses to ND were evoked by endocannabinoids released from pyramidal neurons.

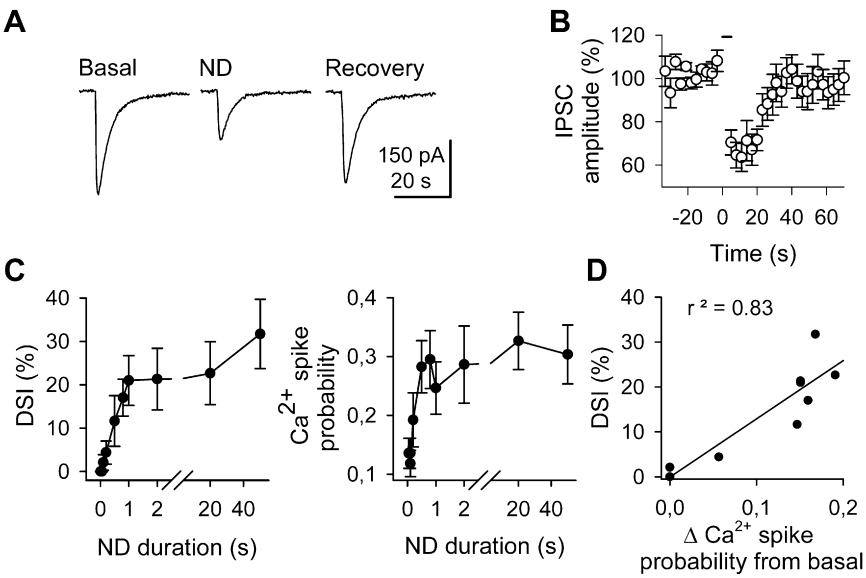

Figure 5. Astrocytic Ca^{2+} Elevations and Endocannabinoid-Mediated DSI Depended on ND Duration

(A) IPSCs before (basal), 3 s after ND, and 20 s later (recovery).

(B) Mean relative IPSC amplitudes (n = 6 neurons). Zero time corresponds to ND (for 5 s; horizontal bar).

(C) Simultaneously recorded DSI and astrocyte Ca^{2+} spike probability evoked at different ND duration ($n \geq 5$ for each point). Error bars indicate SEM.

(D) Corresponding plot of astrocyte Ca^{2+} spike probability change from basal versus DSI. Points were fitted to a linear regression (straight line; $r^2 = 0.83$).

CB1R-Mediated Calcium Elevations in Astrocytes Evoke Glutamate-Mediated Slow Inward Currents in Pyramidal Neurons

We next investigated the physiological consequences of the endocannabinoid-mediated astrocyte Ca^{2+} elevations on neuronal excitability. Recent reports indicate that exogenous experimental stimuli (extracellular application of ATP or the mGluR agonist DHPG, astrocytic depolarization, or photorelease of intracellular Ca^{2+} from Ca^{2+}-caged compounds) that elevate intracellular Ca^{2+} in astrocytes induce glutamate-mediated slow inward currents (SICs) in adjacent neurons (Angulo et al., 2004; Araque et al., 1998; Fellin et al., 2004; Perea and Araque, 2005). We then asked whether endocannabinoids released by pyramidal neurons may serve as endogenous signals that, by elevating the astrocytic Ca^{2+}, stimulate the release of glutamate from astrocytes. We simultaneously recorded whole-cell currents from two nearby pyramidal neurons as well as the Ca^{2+} levels from adjacent astrocytes, in the presence of the cocktail containing neurotransmitter receptor antagonists (except AP5) and TTX and in the absence of extracellular Mg^{2+} to maximize NMDAR activation. Because the observation of SICs during neuronal depolarization was prevented in the stimulating neuron, currents were analyzed in the nonstimulated neuron. Under these conditions, pyramidal neurons displayed a basal frequency of SICs of $1.3 \pm 0.4\ min^{-1}$ (mean SIC amplitude: 34 ± 4 pA; n = 36; cf. Angulo et al., 2004; Fellin et al., 2004; Perea and Araque, 2005). Depolarization of one pyramidal neuron (to 0 mV for 20 s) increased the Ca^{2+} oscillation frequency in astrocytes and concomitantly increased the frequency of SICs in the adjacent neuron (Figure 7). SICs were totally abolished by 50 μM AP5, confirming that they were due to NMDAR activation (Angulo et al., 2004; Fellin et al., 2004; Perea and Araque, 2005), while the Ca^{2+} oscillation frequency increase was unaffected. In contrast, the ND-evoked frequency increase of both Ca^{2+} oscillations and SICs were prevented by 2 μM AM251, which did not significantly modify their basal frequency. In the presence of extracellular Mg^{2+}, the frequency of SICs, detected as AP5-sensitive outward currents at depolarized membrane potentials (>30 mV), was also increased after ND (from 1.4 ± 0.4 to 3.1 ± 0.6; n = 4; Figure 7E), indicating that this phenomenon also occurs under normal extracellular Ca^{2+} and Mg^{2+} concentrations. Altogether, these results indicate that CB1R-mediated Ca^{2+} elevations in astrocytes are required for the SIC frequency increase induced by neuronal depolarization.

Therefore, we hypothesized that these effects were due to stimulation of endocannabinoid release by neuronal depolarization. To test this hypothesis, we included BAPTA in one of the recording pipettes to prevent Ca^{2+} rises and endocannabinoid release from one neuron, while the other neuron remained as a control. Depolarization of the control neuron increased the frequency of both astrocytic Ca^{2+} oscillations and SICs in the adjacent neuron. In contrast, depolarization of the BAPTA-filled neuron did not significantly modify the basal frequency of both parameters (Figure 7D).

To test whether endocannabinoid-mediated Ca^{2+} elevations in astrocytes are necessary to stimulate glutamate release and increase the frequency of SICs, we analyzed the effects of depleting the internal Ca^{2+} stores with thapsigargin. We first tested whether ND-evoked endocannabinoid release still occurred after 30 min incubation with 1 μM thapsigargin by recording IPSCs to monitor the amount of DSI, as indicative of endocannabinoid release. DSI could be observed in thapsigargin (although with a relatively smaller amplitude than in control; cf. Isokawa and Alger, 2006), indicating that ND-evoked endocannabinoid release was not prevented by thapsigargin (Figure 8A). Then, in parallel experiments, we simultaneously recorded whole-cell currents from two pyramidal neurons and Ca^{2+} signals from astrocytes. The ND-evoked increase of both astrocyte Ca^{2+} spike probability and frequency of SICs observed in control conditions, were abolished after incubation with thapsigargin (Figures 8B and 8C). These results indicate that endocannabinoid release from neurons requires astrocytic Ca^{2+} elevations to stimulate glutamate release from astrocytes and increase the frequency of SICs in pyramidal neurons.

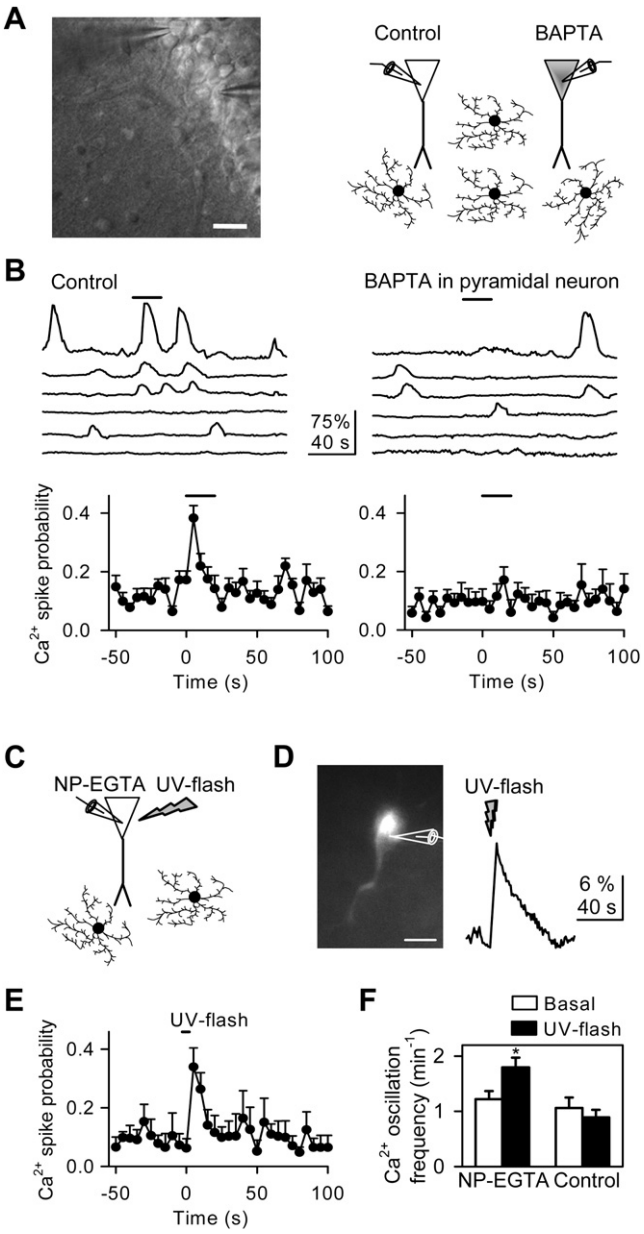

Figure 6. Astrocytic Ca^{2+} Elevations Are Mediated by Endocannabinoids Released from Pyramidal Neurons

(A) Infrared differential interference contrast image and schematic drawing showing simultaneous recording from two pyramidal neurons. One recording pipette included 40 mM BAPTA to prevent Ca^{2+} rises in one pyramidal neuron, while the other neuron was filled with standard intracellular solution (Control). Scale bar, 25 μm.

(B) Representative traces of Ca^{2+} levels from six astrocytes in a typical field of view (top) and astrocyte Ca^{2+} spike probability (bottom) before and after depolarization (horizontal bars) of control and BAPTA-filled neurons (left and right, respectively) (n = 9 slices).

(C) Schematic drawing.

(D) (Left) Image showing fluorescence intensities of NP-EGTA and fluo-4-filled neuron in stratum pyramidale. Scale bar, 15 μm. (Right) Neuron Ca^{2+} levels evoked by UV-flash stimulation in the soma.

(E) Astrocyte Ca^{2+} spike probability versus time (n = 6 slices). Zero time corresponds to the beginning of UV-flash stimulation (horizontal bar).

(F) Mean Ca^{2+} oscillation frequency before (basal) and after UV-flash stimulation of control or NP-EGTA-filled neurons. Error bars indicate SEM. Significant differences were established at *$p < 0.05$.

Taken together, these results indicate that depolarization of neurons stimulates the release of endocannabinoids, which activate CB1Rs in astrocytes, elevating their intracellular Ca^{2+} and inducing the release of glutamate, which in turn serves as a feedback signal activating NMDARs in neurons.

DISCUSSION

The expression of CB1Rs by different neuronal populations is well documented (for reviews see Freund et al., 2003; Piomelli, 2003). However, their expression by astrocytes both in culture and in situ is controversial (e.g., see Stella, 2004). The reported experimental discrepancies may arise from the well-known phenotypic changes of astrocytes in different culture conditions. Nevertheless, although ultrastructural studies detected CB1Rs in astrocytes of specific brain areas (Rodriguez et al., 2001; Salio et al., 2002) and several studies showed CB1Rs in cultured glial cells (Molina-Holgado et al., 2003; Stella, 2004; Walter and Stella, 2003), their functional expression by astrocytes in situ remained unclear. Here we show that hippocampal astrocytes in situ express functional CB1Rs that can play a relevant role in intercellular signaling in the nervous system.

CB1Rs belong to the G protein-coupled seven-transmembrane receptor (GPCR) superfamily (Matsuda et al., 1990). They are preferentially coupled to PTX-sensitive $G_{i/o}$ proteins (Mackie and Hille, 1992; Piomelli, 2003), and they can activate PLC in a PTX-sensitive manner mediated by the $G_{i/o}$ βγ subunits (Filipeanu et al., 1997; Lograno and Romano, 2004; Netzeband et al., 1999; Sugiura et al., 1997). Furthermore, Lauckner et al. (2005) have reported that CB1Rs can also be coupled to $G_{q/11}$ proteins in an agonist-specific manner, because WIN, but no other agonists, activated $G_{q/11}$ and PLC in HEK293 transfected cells and cultured neurons, challenging the classical idea that GPCRs specifically interact with certain types of G proteins. These authors hypothesized that CB1 interaction with $G_{q/11}$ proteins may occur under different conditions, such as during agonist-dependent conformation stabilization of receptors, at elevated receptor occupancy, or when the ratio between $G_{q/11}$ and $G_{i/o}$ proteins is high. If such is the case, present results suggest that interaction of CB1Rs with $G_{q/11}$ proteins may be more favored in astrocytes than in neurons. Moreover, the present demonstration that CB1R activation by endocannabinoids leads to Ca^{2+} mobilization through activation of PLC in a PTX-insensitive manner indicates that CB1Rs can be naturally coupled to $G_{q/11}$ proteins and suggests that the promiscuity of GPCRs and G proteins may be a general phenomenon with physiological bases and consequences.

Several studies have shown the prominent role of CB1Rs triggering different intracellular signaling cascades other than intracellular Ca^{2+} elevations (see Chevaleyre and Castillo, 2003; Freund et al., 2003; Kreitzer and Regehr, 2002). Furthermore, CB1Rs can evoke Ca^{2+} rises by either activation of $G_{i/o}$ βγ proteins (Filipeanu et al., 1997; Lograno and Romano, 2004; Netzeband et al., 1999; Sugiura et al., 1997), L-type Ca^{2+} channel

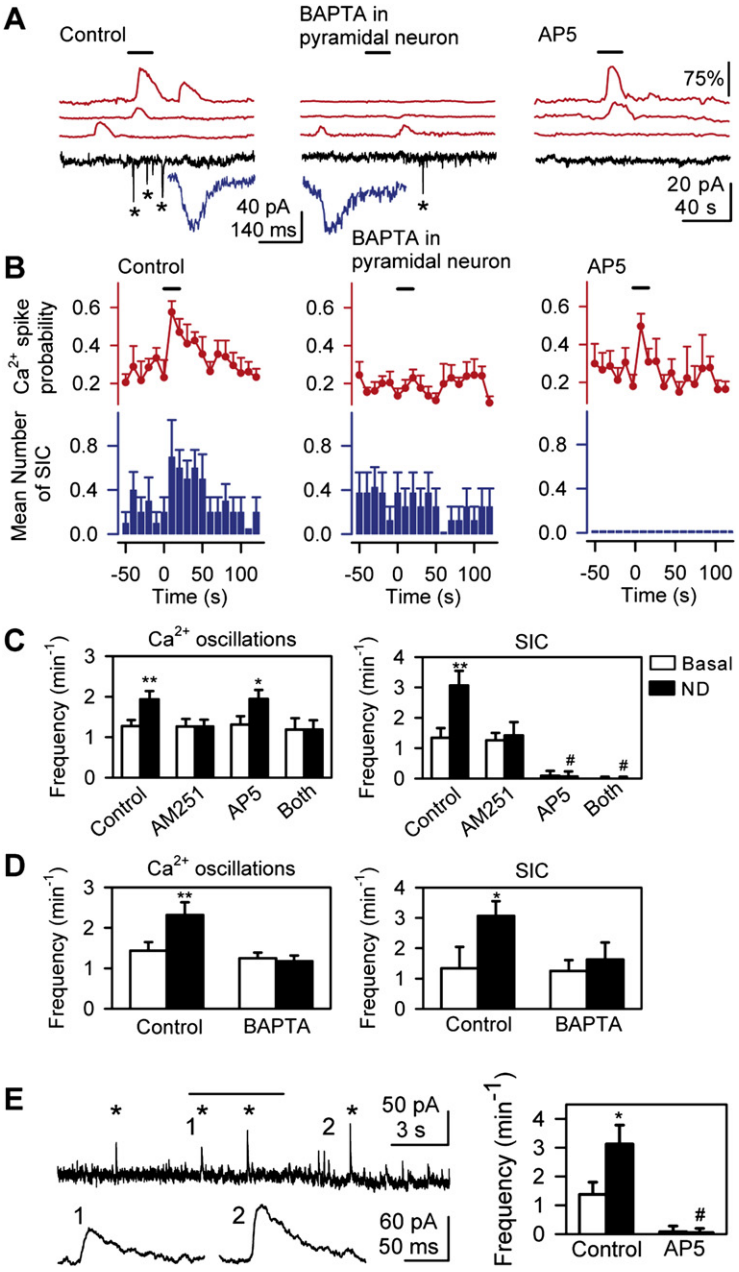

Figure 7. Endocannabinoid-Induced Astrocyte Ca^{2+} Elevations Evoke NMDAR-Mediated SICs in Pyramidal Neurons

(A) Intracellular Ca^{2+} levels from three astrocytes (red traces) and whole-cell currents from adjacent neurons (black and blue traces). The experimental arrangement is as in Figure 6A, i.e., in paired recordings, one neuron was filled with BAPTA, while the other neuron was filled with standard solution (Control). Horizontal bars indicate neuronal depolarization. Recordings were obtained during depolarization of the control neuron (Control), the BAPTA-filled neuron, and the control neuron in the presence of AP5. Asterisks indicate slow inward currents (SICs). Two SICs have been expanded (blue traces).

(B) Astrocyte Ca^{2+} spike probability (red) and mean number of neuronal SICs (blue) before and after neuronal depolarization (horizontal bars) of the control neuron (left), the BAPTA-filled neuron (center), and the control neuron in AP5 (right) (18 paired recorded neurons from n = 9 slices).

(C) Frequency of astrocytic Ca^{2+} oscillations and SICs 50 s before (basal; white bars) and after neuronal depolarization (ND; black bars) of control neurons in control solution and in the presence of AM251, AP5, or both antagonists ($n \geq 5$ slices for each bar).

(D) Frequency of astrocytic Ca^{2+} oscillations and SICs 50 s before (basal; white bars) and after ND (black bars) of control and BAPTA-filled neurons (n = 8 slices).

(E) Whole-cell currents from a pyramidal neuron recorded at +30 mV in the presence of TTX and extracellular Mg^{2+}. SICs detected as outward currents are marked by asterisks, and two SICs have been expanded (lower traces). Frequency of SICs 50 s before (basal; white bars) and after neuronal depolarization (ND; black bars) in control solution and in the presence of AP5 (n = 4 slices for each bar). Error bars indicate SEM. Significant differences were established at $^*p < 0.05$, $^{**}p < 0.01$, and $\#p < 0.001$.

modulation (Rubovitch et al., 2002), or agonist-specific activation of $G_{q/11}$ proteins (Lauckner et al., 2005). Here we have shown that CB1R activation causes astrocyte Ca^{2+} elevations that evoke glutamate-mediated astrocyte-neuron signaling, revealing a physiological role for this CB1R-evoked Ca^{2+} signaling.

Endocannabinoid signaling plays important roles in synaptic function (Alger, 2002; Chevaleyre et al., 2006; Kreitzer and Regehr, 2002; Walter and Stella, 2003). Considering recent data demonstrating the relevance of neuron-astrocyte communication in brain physiology (Araque et al., 2001; Haydon, 2001; Haydon and Carmignoto, 2006; Nedergaard et al., 2003; Perea and Araque, 2007; Volterra and Meldolesi, 2005), whether endocannabinoid signaling between neurons and astrocytes is involved in these processes is an exciting hypothesis that deserves investigation.

Because astrocyte-evoked SICs may influence neuronal excitability and synchronization (Angulo et al., 2004; Araque et al., 1998; Fellin et al., 2004), the endocannabinoid-induced astrocyte-mediated SICs may have a relevant physiological significance on neuronal activity. The fact that SICs are mediated by NMDA receptors, which require the depolarization of the postsynaptic neuron to open under physiological conditions, suggests that this astrocyte-neuron signaling needs the coincidence of neuronal and astrocytic activity.

CB1Rs are known to mediate cannabinoid effects in drug-related behavior (Maldonado et al., 2006). These effects are thought to be mediated by the direct control of neural network activity. However, present evidence raise the possibility that direct activation of CB1Rs in astrocytes may be a primary cause involved in the cannabinoid effects. Hence, the fact that astrocytes express functional CB1Rs must be considered when interpreting the cellular basis of the behavioral effects of cannabinoids.

In conclusion, we provide evidence indicating that astrocytes express CB1Rs that upon activation by endocannabinoids released from pyramidal neurons lead to PLC-dependent Ca^{2+} mobilization from internal stores. This endocannabinoid-induced

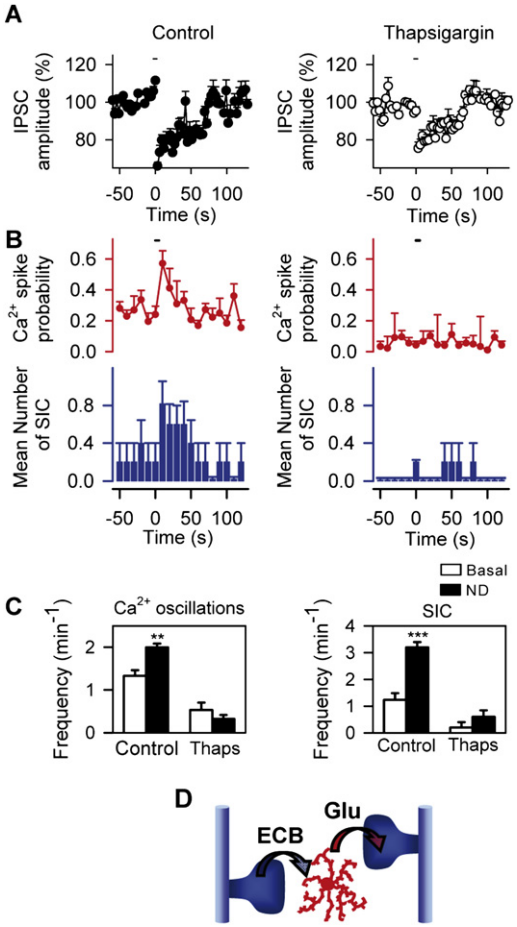

Figure 8. Endocannabinoid-Induced Astrocyte Ca^{2+} Elevations Are Necessary to Evoke SICs in Pyramidal Neurons

(A) IPSC amplitude before and after 5 s ND in control (left) and 1 μM thapsigargin (n = 4). Zero time corresponds to ND (horizontal bar).

(B) Astrocyte Ca^{2+} spike probability (red) and mean number of neuronal SICs (blue) before and after neuronal depolarization (horizontal bars) in control (left) and 1 μM thapsigargin (ten paired recorded neurons from n = 5 slices).

(C) Frequency of astrocytic Ca^{2+} oscillations and SICs 50 s before (basal; white bars) and after ND (black bars) in control and thapsigargin (n = 5 slices). Error bars indicate SEM. Significant differences were established at $^{**}p < 0.01$ and $^{***}p < 0.001$.

(D) Schematic drawing representing the endocannabinoid-mediated neuron-to-astrocyte signaling and the subsequent glutamate-mediated astrocyte-to-neuron signaling.

astrocyte Ca^{2+} signal may signal back to neurons through the release of glutamate that activates NMDARs in pyramidal neurons. These results indicate that neurons and astrocytes communicate via endocannabinoid signaling and suggest the existence of intercellular communication pathways mediated by endocannabinoid-glutamate signaling where astrocytes serve as a bridge for interneuronal communication.

Present results reveal that astrocytes are cellular targets of cannabinoids, identifying these cells as cellular elements possibly involved in the physiology of cannabinoid addiction as well as potential targets for the treatment of cannabinoid-related drug abuse. Furthermore, considering the importance of the endocannabinoid-mediated intercellular signaling in numerous processes of the nervous system, such as pain perception or learning and memory, present findings indicate that astrocytes may be actively involved in relevant phenomena of brain physiology.

EXPERIMENTAL PROCEDURES

Hippocampal Slice Preparation

Acute hippocampal slices were obtained as previously described (Araque et al., 2002; Perea and Araque, 2005). All the procedures for handling and sacrificing animals followed the European Commission guidelines (86/609/CEE) and were supervised by the Instituto Cajal veterinary officer. CD1 and C57BL/6 mice (12–17 days old) were anesthetized and then decapitated. The brain was rapidly removed and placed in ice-cold artificial cerebrospinal fluid (ACSF). Brain slices (350–400 μm thick) were cut with a Vibratome (Pelco 101, Series 1000, St Louis, MO) and incubated during >1 hr at room temperature (21°C–24°C) in ACSF. The ACSF contained (in mM) NaCl 124, KCl 2.69, KH_2PO_4 1.25, $MgSO_4$ 2, $NaHCO_3$ 26, $CaCl_2$ 2, and glucose 10 and was gassed with 95% O_2/5% CO_2 (pH = 7.3). Slices were then transferred to an immersion recording chamber and superfused with gassed ACSF. In experiments designed to optimize NMDAR activation, the extracellular Mg^{2+} was equimolarly substituted by Ca^{2+}, and 10 μM glycine was added. Cells were visualized under an Olympus BX50WI microscope (Olympus Optical, Tokyo, Japan) equipped with infrared and differential interference contrast imaging devices and with a 40× water-immersion objective. In some cases, slices from CB1 receptor knockout mice, generously donated by Dr. A. Zimmer, were used (Zimmer et al., 1999).

Electrophysiology

Electrophysiological recordings of CA1 hippocampal pyramidal neurons and astrocytes were made using the whole-cell patch-clamp technique. Patch electrodes were fabricated from borosilicate glass capillaries and had resistances of 6–10 MΩ when filled with the internal solution that contained (in mM) $KMeSO_4$ 100, KCl 50, HEPES 10, ATP-Na_2 4 (pH = 7.3). Recordings were obtained with PC-ONE amplifiers (Dagan Instruments, Minneapolis, MN). Fast and slow whole-cell capacitances were neutralized, series resistance was compensated (about 70%), and the membrane potential was held at −60 mV, unless stated otherwise. Signals were fed to a Pentium-based PC through a DigiData 1320 interface board (Axon Instruments). pCLAMP 8 software (Axon Instruments) was used for stimulus generation, data display, acquisition, and storage. In some experiments, we performed paired whole-cell recordings from two CA1 pyramidal neurons (distance of the somas <100 μm). Astrocytes were identified according to morphological and electrophysiological criteria (e.g., Araque et al., 2002; Bergles et al., 2000; Bezzi et al., 1998; Pasti et al., 1997; Perea and Araque, 2005) (Figure S2). ND experiments started <30 min after entering whole-cell configuration. To test the ND effects on the SIC frequency, the number of SICs recorded from each neuron during 50 s periods before (basal) and after the onset of the ND were compared. To illustrate the time course of the effects of ND on the appearance of SICs in Figure 7B, the number of SICs were grouped in 5 s bins, and the mean number of SICs for each bin was calculated by averaging the values obtained from 16 paired recorded neurons from eight slices. Experiments were performed at room temperature (22°C–24°C), unless stated otherwise. Data are expressed as mean ± SEM. Statistical differences were established by the Student's t test.

Synaptic currents recorded from pyramidal neurons were evoked using bipolar nichrome wire electrodes (80 μm diameter) that were connected to a stimulator through isolation units (Grass S88, Quincy, MA) and placed in the stratum radiatum near the border of the CA1 pyramidal neurons. IPSCs were isolated in the presence of 20 μM CNQX and 50 μM AP5. Continuous stimuli were delivered at 0.3 Hz. DSI was quantified from the mean amplitude of three IPSCs after ND relative to the mean amplitude of 20 IPSCs before ND (basal). Only slices in which the recorded neuron showed DSI after 5 s ND were considered.

Calcium Imaging

Ca^{2+} levels in astrocytes located in the stratum radiatum of the CA1 region of the hippocampus were monitored by fluorescence microscopy using the Ca^{2+}

indicator fluo-4 (Molecular Probes, Eugene, OR). Slices were incubated with fluo-4-AM (2–5 μl of 2 mM dye were dropped over the hippocampus, attaining a final concentration of 2–10 μM and 0.01% of pluronic) for 20–30 min at room temperature. Under these conditions, most of the cells loaded were astrocytes (Araque et al., 2002; Kang et al., 1998; Nett et al., 2002; Parri et al., 2001; Perea and Araque, 2005), as confirmed in some cases by their electrophysiological properties (see Figure S2). In some cases, Ca^{2+} levels in single astrocytes were monitored by including fluo-4 in the recording pipette (Figures S2B and S2C). Astrocytes were imaged using a CCD camera (Retiga EX; Qimaging, Canada) attached to the Olympus microscope. Cells were illuminated during 200–500 ms with a xenon lamp at 490 nm using a monochromator Polychrome II (T.I.L.L. Photonics, Planegg, Germany), and images were acquired every 0.5–2 s. The monochromator Polychrome II and the CCD camera were controlled and synchronized by the IP Lab software (BD Biosciences, MD) that was also used for quantitative epifluorescence measurements. Ca^{2+} variations recorded at the soma of the cells were estimated as changes of the fluorescence signal over baseline ($\Delta F/F_0$), and regions of interest were considered to respond to the stimulation when $\Delta F/F_0$ increased three times the standard deviation of the baseline for at least two consecutive images and with a delay $\leq$15 s after the stimulation.

The astrocyte Ca^{2+} signal was quantified from the probability of occurrence of a Ca^{2+} spike and the Ca^{2+} oscillation frequency. The Ca^{2+} spike probability was calculated from the number of Ca^{2+} elevations grouped in 5 s bins recorded from 6 to 14 astrocytes in the field of view. The time of occurrence was considered to be the onset of the Ca^{2+} spike. The Ca^{2+} oscillation frequency was obtained from the number of Ca^{2+} spikes occurring in 6 to 14 astrocytes in the field of view during 50 s periods before (basal) and after the onset of the neuronal depolarization. To test the effects of ND on Ca^{2+} spike probability under different conditions, the respective mean basal (50 s before ND) and maximum Ca^{2+} spike probability (i.e., 5–10 s after ND) from different slices were averaged and compared. Mean values were obtained from at least four slices in each condition.

UV-Flash Photolysis

In photostimulation experiments, pyramidal neurons were recorded with patch pipettes filled with the internal solution containing 50 μM fluo-4 and 5 mM NP-EGTA. For Ca^{2+} uncaging, train pulses (1 ms duration, 6–15 mW) of UV light (340–380 nm) were delivered at 2 Hz during 5 s to the soma (optical window of 15–25 μm diameter) using a flash photolysis system (Rapp OptoElectronic, Hamburg, Germany).

Immunocytochemistry

Anesthetized mice were perfused transcardially with 4% paraformaldehyde in 0.1 M phosphate buffer (PB). Brains were removed and postfixed in 4% paraformaldehyde in 0.1 M PB for 3 hr. Coronal slices (35 μm thick) were cut with a vibratome and processed to visualize the expression of CB1Rs and GFAP on astrocytes. Slices were preincubated in 0.25% Triton X-100 with 3% normal goat serum in PB during 2 hr, then were transferred to a new solution including both rabbit polyclonal CB1R (dilution 1:250; Affinity Bioreagents) and mouse monoclonal anti-GFAP-Cy3 conjugate antibody. Sections were incubated for 24 hr at 4°C, rinsed in 0.1 M PB, and transferred to a solution containing the secondary antibody, Alexa 488-conjugated goat anti-rabbit IgG (1:1000; Molecular Probes). After washing, slices were mounted in glycerol (50% in PB) and examined using laser-scanning confocal microscopy. Control experiments for immunocytochemistry were performed in the absence of primary antibody for CB1Rs, and no significant staining was detected under these control conditions.

Drugs

N-(piperidin-1-yl)-5-(4-iodophenyl)-1-(2,4-dichlorophenyl)-4-methyl-1H-pyrazole-3-carboxamide (AM-251), arachidonylethanolamide (AEA), 6-cyano-7-nitroquinoxaline-2,3-dione(CNQX), D(-)-2-amino-5-phosphonopentanoic acid (AP5), 2-methyl-6-(phenylethynyl)pyridine hydrochloride (MPEP), 2-arachidonylglycerol (2AG), (S)-(+)-α-amino-4-carboxy-2-methylbenzeneacetic acid (LY), (RS)-3-amino-2-(4-chlorophenyl)propylsulfonic acid (saclofen), and (R)-(+)-methanandamide (MAEA) were purchased from Tocris Cookson (Bristol, UK). Tetrodotoxin (TTX) was acquired from Alomone Labs (Jerusalem, Israel). Fluo-4-AM (Molecular Probes, Eugene, OR). All other drugs were from Sigma.

WIN, 2AG, AEA, and MAEA were delivered by 2–5 s duration pressure pulses (PMI-100 DAGAN, Minneapolis, MN) using a pulled capillary filled with WIN (30–300 μM), 2AG (100 μM), AEA (300 μM), and MAEA (300 μM), dissolved in ACSF. Based on quantification of the Alexa 594 fluorescence, we calculated the pressure-ejected volume as ~33 pl, and we estimated a ~67% dilution of the pipette solution in 100 μm^3, which resulted in a final agonist concentration within the usual range of action (e.g., WIN concentration around the recorded cell was ~1–10 μM). GABA (700 mM) was ionophoretically delivered. Ionophoretical and pressure pulse experiments were performed in 1 μM TTX.

SUPPLEMENTAL DATA

The Supplemental Data for this article can be found online at http://www.neuron.org/cgi/content/full/57/6/883/DC1/.

ACKNOWLEDGMENTS

We thank G. Perea for her valuable assistance; W. Buño, C. Guaza, E.D. Martín, and M. Fuenzalida for critical comments on the manuscript; J. García-Marqués, A. Muñoz, and L. Mestre for their help with immunocytochemistry; and A. Zimmer for the generous gift of the CB1R knockout mice. This work was supported by grants from MEC (BFU2004-00448; BFU2007-64764), Comunidad de Madrid - CSIC (200620M083), Spain, and European Union (HEALTH-F2-2007-202167). M.N. is a FPI-MEC predoctoral fellow.

Received: July 2, 2007
Revised: November 19, 2007
Accepted: January 10, 2008
Published: March 26, 2008

REFERENCES

Alger, B.E. (2002). Retrograde signaling in the regulation of synaptic transmission: focus on endocannabinoids. Prog. Neurobiol. *68*, 247–286.

Angulo, M.C., Kozlov, A.S., Charpak, S., and Audinat, E. (2004). Glutamate released from glial cells synchronizes neuronal activity in the hippocampus. J. Neurosci. *24*, 6920–6927.

Araque, A., Parpura, V., Sanzgiri, R.P., and Haydon, P.G. (1998). Glutamate-dependent astrocyte modulation of synaptic transmission between cultured hippocampal neurons. Eur. J. Neurosci. *10*, 2129–2142.

Araque, A., Parpura, V., Sanzgiri, R.P., and Haydon, P.G. (1999). Tripartite synapses: glia, the unacknowledged partner. Trends Neurosci. *22*, 208–215.

Araque, A., Carmignoto, G., and Haydon, P.G. (2001). Dynamic signaling between neurons and glia. Annu. Rev. Physiol. *63*, 795–813.

Araque, A., Martin, E.D., Perea, G., Arellano, J.I., and Buño, W. (2002). Synaptically released acetylcholine evokes Ca2+ elevations in astrocytes in hippocampal slices. J. Neurosci. *22*, 2443–2450.

Beattie, E.C., Stellwagen, D., Morishita, W., Bresnahan, J.C., Ha, B.K., Von Zastrow, M., Beattie, M.S., and Malenka, R.C. (2002). Control of synaptic strength by glial TNFα. Science *295*, 2282–2285.

Bergles, D.E., Roberts, J.D., Somogyi, P., and Jahr, C.E. (2000). Glutamatergic synapses on oligodendrocyte precursor cells in the hippocampus. Nature *40*, 187–191.

Bezzi, P., Carmignoto, G., Pasti, L., Vesce, S., Rossi, D., Rizzini, B.L., Pozzan, T., and Volterra, A. (1998). Prostaglandins stimulate calcium-dependent glutamate release in astrocytes. Nature *391*, 281–285.

Catsicas, M., and Mobbs, P. (2001). GABAb receptors regulate chick retinal calcium waves. J. Neurosci. *21*, 897–910.

Chevaleyre, V., and Castillo, P.E. (2003). Heterosynaptic LTD of hippocampal GABAergic synapses: a novel role of endocannabinoids in regulating excitability. Neuron *38*, 461–472.

Chevaleyre, V., Takahashi, K.A., and Castillo, P.E. (2006). Endocannabinoid-mediated synaptic plasticity in the CNS. Annu. Rev. Neurosci. *29*, 37–76.

Di Marzo, V., Bifulco, M., and De Petrocellis, L. (2004). The endocannabinoid system and its therapeutic exploitation. Nat. Rev. Drug Discov. *3*, 771–784.

Fellin, T., Pascual, O., Gobbo, S., Pozzan, T., Haydon, P.G., and Carmignoto, G. (2004). Neuronal synchrony mediated by astrocytic glutamate through activation of extrasynaptic NMDA receptors. Neuron *43*, 729–743.

Filipeanu, C.M., de Zeeuw, D., and Nelemans, S.A. (1997). Delta9-tetrahydrocannabinol activates [Ca2+]i increases partly sensitive to capacitative store refilling. Eur. J. Pharmacol. *336*, R1–R3.

Freund, T.F., Katona, I., and Piomelli, D. (2003). Role of endogenous cannabinoids in synaptic signalling. Physiol. Rev. *83*, 1017–1066.

Haydon, P.G. (2001). GLIA: listening and talking to the synapse. Nat. Rev. Neurosci. *2*, 185–193.

Haydon, P.G., and Carmignoto, G. (2006). Astrocyte control of synaptic transmission and neurovascular coupling. Physiol. Rev. *86*, 1009–1031.

Isokawa, M., and Alger, B.E. (2006). Ryanodine receptor regulates endogenous cannabinoid mobilization in the hippocampus. J. Neurophysiol. *95*, 3001–3011.

Kang, J., Jiang, L., Goldman, S.A., and Nedergaard, M. (1998). Astrocyte-mediated potentiation of inhibitory synaptic transmission. Nat. Neurosci. *1*, 683–692.

Kreitzer, A.C., and Regehr, W.G. (2001). Retrograde inhibition of presynaptic calcium influx by endogenous cannabinoids at excitatory synapses onto Purkinje cells. Neuron *29*, 717–727.

Kreitzer, A.C., and Regehr, W.G. (2002). Retrograde signaling by endocannabinoids. Curr. Opin. Neurobiol. *12*, 324–330.

Kreitzer, A.C., Carter, A.G., and Regehr, W.G. (2002). Inhibition of interneuron firing extends the spread of endocannabinoid signaling in the cerebellum. Neuron *34*, 787–796.

Lauckner, J.E., Hille, B., and Mackie, K. (2005). The cannabinoid agonist WIN55,212–2 increases intracellular calcium via CB1 receptor coupling to Gq/11 G proteins. Proc. Natl. Acad. Sci. USA *102*, 19144–19149.

Llano, I., Leresche, N., and Marty, A. (1991). Calcium entry increases the sensitivity of cerebellar Purkinje cells to applied GABA and decreases inhibitory synaptic currents. Neuron *6*, 565–574.

Lograno, M.D., and Romano, M.R. (2004). Cannabinoid agonists induce contractile responses through Gi/o-dependent activation of phospholipase C in the bovine ciliary muscle. Eur. J. Pharmacol. *494*, 55–62.

Mackie, K., and Hille, B. (1992). Cannabinoids inhibit N-type calcium channels in neuroblastoma-glioma cells. Proc. Natl. Acad. Sci. USA *89*, 3825–3829.

Maldonado, R., Valverde, O., and Berrendero, F. (2006). Involvement of the endocannabinoid system in drug addiction. Trends Neurosci. *29*, 225–232.

Matsuda, L.A., Lolait, S.J., Brownstein, M.J., Young, A.C., and Bonner, T.I. (1990). Structure of a cannabinoid receptor and functional expression of the cloned cDNA. Nature *346*, 561–564.

Molina-Holgado, F., Pinteaux, E., Moore, J.D., Molina-Holgado, E., Guaza, C., Gibson, R.M., and Rothwell, N.J. (2003). Endogenous interleukin-1 receptor antagonist mediates anti-inflammatory and neuroprotective actions of cannabinoids in neurons and glia. J. Neurosci. *23*, 6470–6474.

Munro, S., Thomas, K., and Abu-Shaar, M.L. (1993). Molecular characterization of a peripheral receptor for cannabinoids. Nature *365*, 61–65.

Nedergaard, M., Ransom, B., and Goldman, S.A. (2003). New roles for astrocytes: Redefining the functional architecture of the brain. Trends Neurosci. *26*, 523–530.

Nett, W.J., Oloff, S.H., and McCarthy, K.D. (2002). Hippocampal astrocytes in situ exhibit calcium oscillations that occur independent of neuronal activity. J. Neurophysiol. *87*, 528–537.

Netzeband, J.G., Conroy, S.M., Parsons, K.L., and Gruol, D.L. (1999). Cannabinoids enhance NMDA-elicited Ca2+ signals in cerebellar granule neurons in culture. J. Neurosci. *19*, 8765–8777.

Ohno-Shosaku, T., Maejima, T., and Kano, M. (2001). Endogenous cannabinoids mediate retrograde signals from depolarized postsynaptic neurons to presynaptic terminals. Neuron *29*, 729–738.

Parri, H.R., Gould, T.M., and Crunelli, V. (2001). Spontaneous astrocytic Ca2+ oscillations in situ drive NMDAR-mediated neuronal excitation. Nat. Neurosci. *4*, 803–812.

Pasti, L., Volterra, A., Pozzan, T., and Carmignoto, G. (1997). Intracellular calcium oscillations in astrocytes: a highly plastic, bidirectional form of communication between neurons and astrocytes in situ. J. Neurosci. *17*, 7817–7830.

Perea, G., and Araque, A. (2005). Properties of synaptically evoked astrocyte calcium signal reveal synaptic information processing by astrocytes. J. Neurosci. *25*, 2192–2203.

Perea, G., and Araque, A. (2007). Astrocytes potentiate transmitter release at single hippocampal synapses. Science *317*, 1083–1086.

Piomelli, D. (2003). The molecular logic of endocannabinoid signalling. Nat. Rev. Neurosci. *4*, 873–884.

Porter, J.T., and McCarthy, K.D. (1996). Hippocampal astrocytes in situ respond to glutamate released from synaptic terminals. J. Neurosci. *16*, 5073–5081.

Porter, J.T., and McCarthy, K.D. (1997). Astrocytic neurotransmitter receptors in situ and in vivo. Prog. Neurobiol. *51*, 439–455.

Rodriguez, J.J., Mackie, K., and Pickel, V.M. (2001). Ultrastructural localization of the CB1 cannabinoid receptor in mu-opioid receptor patches of the rat Caudate putamen nucleus. J. Neurosci. *21*, 823–833.

Rubovitch, V., Gafni, M., and Sarne, Y. (2002). The cannabinoid agonist DALN positively modulates L-type voltage-dependent calcium-channels in N18TG2 neuroblastoma cells. Brain Res. *101*, 93–102.

Salio, C., Doly, S., Fischer, J., Franzoni, M.F., and Conrath, M. (2002). Neuronal and astrocytic localization of the cannabinoid receptor-1 in the dorsal horn of the rat spinal cord. Neurosci. Lett. *329*, 13–16.

Serrano, A., Haddjeri, N., Lacaille, J.C., and Robitaille, R. (2006). GABAergic network activation of glial cells underlies hippocampal heterosynaptic depression. J. Neurosci. *26*, 5370–5382.

Stella, N. (2004). Cannabinoid signaling in glial cells. Glia *48*, 267–277.

Sugiura, T., Kodaka, T., Kondo, S., Nakane, S., Kondo, H., Waku, K., Ishima, Y., Watanabe, K., and Yamamoto, I. (1997). Is the cannabinoid CB1 receptor a 2-arachidonoylglycerol receptor? Structural requirements for triggering a Ca2+ transient in NG108–15 cells. J. Biochem. (Tokyo) *122*, 890–895.

Volterra, A., and Bezzi, P. (2002). The Tripartite Synapse: Glia. In Synaptic Transmission, A. Volterra, P.J. Magistretti, and P.G. Haydon, eds. (New York: Oxford University Press), pp. 164–184.

Volterra, A., and Meldolesi, J. (2005). Astrocytes, from brain glue to communication elements: the revolution continues. Nat. Rev. Neurosci. *6*, 626–640.

Walter, L., and Stella, N. (2003). Endothelin-1 increases 2-arachidonoyl glycerol (2-AG) production in astrocytes. Glia *44*, 85–90.

Wilson, R.I., and Nicoll, R.A. (2001). Endogenous cannabinoids mediate retrograde signalling at hippocampal synapses. Nature *410*, 588–592.

Wilson, R.I., and Nicoll, R.A. (2002). Endocannabinoid signaling in the brain. Science *296*, 678–682.

Zimmer, A., Zimmer, A.M., Hohmann, A.G., Herkenham, M., and Bonner, T.I. (1999). Increased mortality, hypoactivity, and hypoalgesia in cannabinoid CB1 receptor knockout mice. Proc. Natl. Acad. Sci. USA *96*, 5780–5785.